JOURNAL OF MATERIALS SCIENCE 32 (1997) 1717–1724

Densification process of TiC_x–Ni composites formed by self-propagating high-temperature synthesis reaction

YONG CHOI
Department of Metallurgical Engineering, Sun Moon University, Asan-City, Chung-Nam, 336-840 Korea

J. K. LEE, M. E. MULLINS*
*Department of Metallurgical and Materials Engineering, and *Department of Chemical Engineering, Michigan Technological University, Houghton, MI 49931, USA*

Densification behaviour of the TiC–Ni system formed by self-propagating high-temperature synthesis (SHS) were studied to develop the structural metal-matrix composites. The composites were prepared by two routes: (1) consolidation during the SHS reaction, and (2) consolidation process after the SHS reaction. The final phases of the stoichiometric reactant mixture of titanium and graphite with 50 wt% nickel produced by simultaneous combustion reactions, were titanium carbide in a nickel-rich solid solution containing carbon and titanium. The density of the products was relatively low, with a value of 90% theoretical density. In the second approach, liquid infiltration and liquid-phase sintering were applied for the titanium carbide–nickel mixture. Densification rates were reduced due to the excess carbon in the combustion products of titanium carbide. The densities of the liquid-phase sintered samples were more than 97% theoretical density.

1. Introduction

Self-propagating high-temperature synthesis (SHS) is a combustion process characterized by an exothermic heat release sufficient to propagate a combustion front through the powder compact, completely consuming the reactant powders once ignition is achieved. It has the advantages of high-purity products, potential for non-equilibrium products and no high-temperature furance process. One of the major drawbacks in the SHS products is the highly porous nature of the products. This porosity in the products can be the result of the contribution from one or more of the following factors: the existing porosity in the reactants, the difference in the molar volume between reactants and products, gas evolution during the combustion reaction and thermal migration of vacancies [1]. In order to produce a dense material, some type of densification process must be included in the fabrication process to make a structural metal matrix composite. There are two methods for obtaining dense combustion products: (1) consolidation during the self-propagating high-temperature synthesis reaction, and (2) consolidation processing in a second step after the self-propagating high-temperature synthesis reaction. The former is attractive because it combines the synthesis and the densification into a one step process.

Maksimov *et al.* have studied the TiB_2-Fe system [2]. This work considered the possibility of reacting elemental titanium, amorphous boron, and carbonyl iron by the combustion region to form titanium boride–iron composites. The synthesis conditions were chosen so that after passage of the combustion front, the product would consist of a large quantity of titanium diboride grains in the melt. The density of the final products could be increased by decreasing the combustion temperature and by subjecting the reactants to a thermal vacuum treatment prior to ignition. By lowering the melting point of the product phase, finely dispersed titanium diboride (~ 1 μm) in an iron matrix was obtained. Taeoka *et al.* [3] fabricated TiB_2–Al composites through the combustion synthesis reaction of Ti–B–Al. The finely dispersed titanium diboride was synthesized by reacting a mixture of titanium, aluminium and amorphous boron powders. The grain size of the titanium diboride formed was less than 0.5 μm, which became smaller as the amount of aluminium increased. They observed that titanium diboride formed in the mixture of Ti–Al–2B; aluminium diboride was not produced during the process of combustion propagation, which suggested that titanium diboride decomposed at a high temperature by a reaction with aluminium, lowering the temperature behind the combustion front. One outstanding work to obtain dense self-propagating high-temperature synthesis products was carried out by Holt and Munior [4]. They studied Ti–C–Ni–Al system and

0022–2461

obtained a combustion product with 99% theoretical density by rapidly heating a mixture of elemental titanium, carbon, nickel and aluminium powders in a graphite die up to the ignition temperature of about 800 °C, and applying mechanical pressure during the combustion reaction. However, it should be noted that this method has shown problems with undersirable phases, due to complex reactions among the initial reactants. Dunmead *et al.* [5] reported that TiC–Ni cermets were formed using combustion synthesis. The spherical titanium carbide was observed in a nickel matrix. By measuring the apparent activation energies from the relation of the combustion front velocity and combustion temperature, they proposed that the formation of titanium carbide in a nickel matrix took place by two mechanisms. (1) At high temperature, a solution and precipitation mechanism was predominant, and (2) at low temperature, a carburization mechanism was dominant. They suggested, that it was not clear whether the combustion reaction was self-propagated throughout the entire sample, because the nickel matrix acted as a diluent in the combustion reaction between titanium and carbon, although titanium nickel intermetallics have a small exothermic heat of formation.

The second method, although it is not a one-step process, seems to control the microstructure and phases of the final products effectively. Liquid-phase sintering and liquid-infiltration methods are low-cost fabrication processes that are effective in obtaining highly dense materials [6, 7]. During this process, the surface free-energy of a particulate system is reduced at an elevated temperature in the presence of a liquid phase. The reduction of free energy is manifested in densification and changes in grain size and shape. The difference between the liquid-phase sintering and the liquid-infiltration method is that infiltration is a two-step variant of liquid-phase sintering. Infiltration starts with a preformed rigid compact usually formed by solid-state sintering. Liquid is introduced into a solid skeleton from the external reservoir, and filling the pores with the liquid phase relied on capillary forces [8]. The resulting microstructure lacks pores and appears similar to other liquid-phase sintered materials. Because the final products of self-propagating high-temperature synthesis reaction are porous skeletons, they are used as a preformed rigid compact.

Hence, in this study, two different densification processes were considered: (1) simultaneous combustion reaction and consolidation, and (2) combustion reaction followed by liquid-phase sintering. In the first approach, emphasis was placed on examining the final phases of the combustion products because the added matrix materials act as a diluent, and complicated reactions are expected during a combustion reaction. In the second approach, emphasis was in the effect of the residual carbon on the densification of titanium carbide nickel composites during liquid-phase sintering because non-stoichiometric titanium carbide, with an amount of carbon remaining inside, was formed in the combustion reaction [9]. The possibility of fabricating metal-matrix composites by combining the self-propagating high-temperature synthesis method with a liquid infiltration method was also considered.

2. Experimental procedure

Titanium, nickel and graphite powders were examined to ascertain the densification behaviour of the combustion products. The titanium powders and nickel powders were less than 325 mesh in size and 99.5% and 99.9% pure, respectively (Aesar, NH, USA). The graphite powders were less than 1 μm diameter (Aldrich, WI, USA). These powders were handled in fume hoods and in a glove box to minimize exposure (< 0.1 p.p.m. hydrogen and < 0.2 p.p.m. oxygen). Stoichiometric amounts of titanium powders and graphite powders were weighed on an electron balance inside a glove box. Each titanium and graphite mix were mechanically blended by a ball mill in *n*-hexane solution, maintaining the stoichiometric compounds. After blending the mixture for 1 h, the sample was dried 12 h in a vacuum atmosphere. The matrix powders were blended into the titanium graphite mixture by a blender in an inert argon atmosphere prior to the self-propagating high-temperature synthesis reaction. The reactant mixture was usually compressed at 28 kPa by a hydraulic press. The resulting compact was preheated up to 300 °C in an electrical furnace before ignition. The ignition was carried out in an inert argon atmosphere (< 0.2 p.p.m. oxygen). A low-power arc ignition source was supplied for only a short time, about 1 s, to prevent significant additional preheating effects on the sample. While the reaction front was propagating, the combustion temperature of the reactant was measured with a Capintec two-wavelength infrared optical pyrometer. In addition, the temperature profiles were monitored by a high-temperature tungsten–rhenium thermocouple attached to a chart recorder. The composition of the final product was analysed with an X-ray diffractometer (Rikoku 100). The details of the experimental apparatus have been presented elsewhere [10].

For liquid-infiltration of nickel matrix into titanium carbide, titanium carbide skeleton and nickel green compact were prepared by self-propagating high-temperature synthesis reaction and cold compaction of nickel powders, respectively. The carbon content in the skeleton was analysed with a carbon/sulfur determinator (LECO CS-244). The accuracy of this instrument is specified at 0.002 wt % C for carbon contents up to 5.0 wt %. The green compact had a size of 1.25 cm × 2.5 cm × 0.5 cm and a density of greater than 60% theoretical density. A high temperature resistance furnace was used for the infiltration process at the temperature of 1420, 1450 and 1500 °C for 10, 120 and 180 min. After liquid-phase sintering, the densities of the metal-matrix composites were determined with a helium gas autopycrometer (Micromeritics, autopycrometer 1320). Microstructural analysis was performed with an optical microscope. Specimens for the optical metallography were prepared by sectioning, mounting, grinding through a series of emery papers ending with 600 grit, and polishing with 6 and 0.25 μm diamond pastes followed by a final

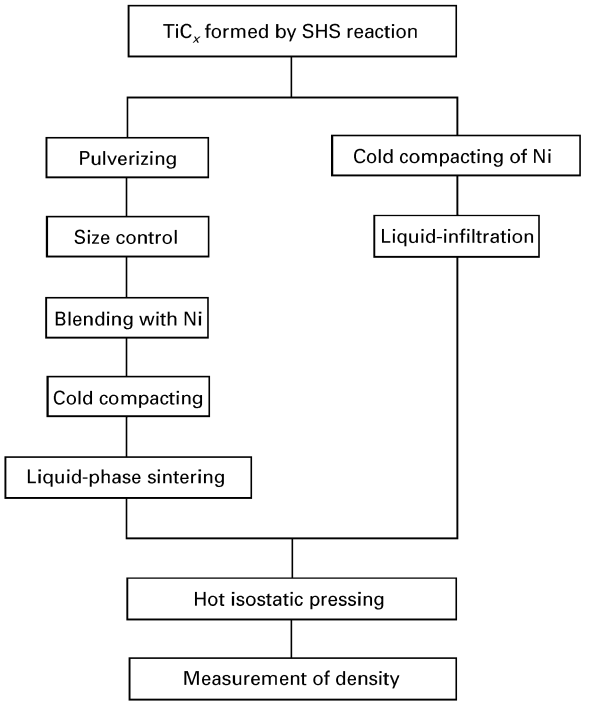

Figure 1 Block diagram for the fabrication process of metal-matrix composites.

polishing using 0.05 μm alumina powders. The samples were then etched with Murakami's solution ($K_3Fe(CN)_6 : NaOH : H_2O = 10\,g : 10\,g : 100\,ml$). Fig. 1 is the block diagram of the fabrication processes of metal-matrix composites with combustion product, titanium carbide.

3. Results and discussion

3.1. Phase identification of SHS products

In order for a one-step fabrication process of metal matrix composites by SHS reaction to be feasible, the combustion front should propagate well. Propagation of the combustion wave depends on combustion temperature, which is experimentally controlled with the addition of a third element into the combustion reaction and preheating of the reactants [11]. Both of these factors, adding a third element and preheating, significantly influence the velocity and temperature of the combustion wave. Accordingly, the measurement of the wave velocity and the combustion temperature, together with preheating and the amount of added elements can provide useful information for determining the feasibility of the one-step process for a given system. Table I shows the maximum combustion temperature and average propagation rates for the various compositions of the reactant powder mixtures.

As shown in the table, the combustion reaction does not self-propagate for the mixture of titanium and graphite with the addition of 50 wt % nickel with a low arc source (500 W) for a short time (1–2 s). However, the combustion reaction was ignited with a high arc source (3 kW) even for the sample with 50 wt % nickel addition. This means that the combustion reaction for the system with nickel addition needs additional heat to sustain the self-propagation high-

TABLE I Composition of reactant powder mixtures, measured average maximum temperatures, and average propagation rates

Specimen number	Composition (mol %)			T_{max}(°C)	Velocity (mm s^{-1})
	Ti	C	Ni		
1	80.0	20.0	0.0	2638	9.8
2	72.8	18.2	10.0	2245	4.2
3	40.0	10.0	50.0	1982	3.0

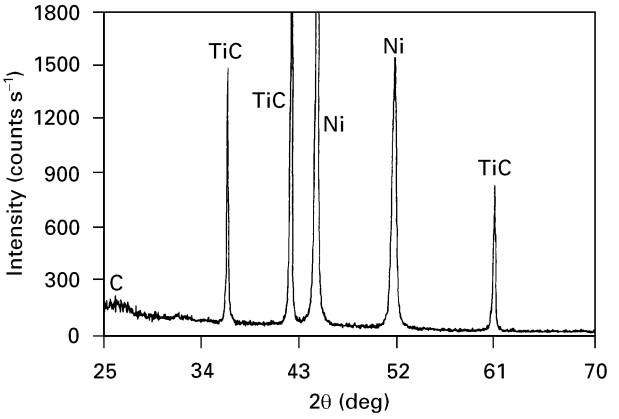

Figure 2 X-ray diffraction pattern of the SHS product formed by the simultaneous reaction with a high-power ignition source (3 kW): the initial stoichiometric mixture of titanium and graphite contains 50 wt % Ni.

TABLE II Lattice constants of TiC$_x$–Ni composites formed by self-propagating high-temperature synthesis with a high-power arc source

Specimen number	Ni content in reactant (wt %)	Lattice constant (nm)	
		TiC$_x$	Ni matrix
1	0.0	0.43276	–
2	10	0.43277	0.35395
3	30	0.43279	0.35614

temperature reaction. Fig. 2 shows an X-ray diffraction pattern for the combustion product of titanium and carbon containing 50 wt % nickel. This pattern shows that the product involves titanium carbide, graphite and nickel, but no trace of free titanium and titanium nickel intermetallic phases remaining after the combustion reaction. Compared with the standard nickel pattern, peak broadening and the phase shift in the nickel spectra were observed in the figure. Lattice constants for the titanium carbide and nickel phases were calculated from X-ray diffraction data, and the results are given in Table II.

Although the absolute value of the lattice parameter determined by X-ray diffraction data has relatively low accuracy, the lattice parameter of the titanium carbide observed was 0.432 79 nm, which was very similar to the value of the product without nickel addition: however, the lattice parameter of the nickel matrix was 0.035 614 nm, which was increased with respect to pure nickel, 0.035 210 nm. This result can be

explained by the solubility of carbon or titanium in nickel. From the equilibrium phase diagram of the nickel–carbon system, the maximum solubility of carbon in nickel is 2.6 mol % at 1316 °C, and the maximum solubility of titanium in nickel is 10.3 mol % at 1306 °C [12]. Because the combustion temperature was at least 1600 °C, as shown in Table I, which was above the eutectic temperatures of nickel–carbon and nickel–titanium systems, large amounts of carbon and titanium atoms were able to dissolve into nickel during the combustion reaction. Considering the isoparametric contour for nickel solid solution of a Ni–Ti–C system at 1260 °C [13], the lattice parameter of nickel solid solution increases up to 0.35 544 nm which is below the observed value, 0.35 614 nm. This may suggest that the observed nickel phase is γ-phase (nickel-rich phase). Singleton and Nash reported that the change of lattice parameter of nickel with carbon content is as follows, $a_0 = 3.524 + 0.0074$ mol % C [13]. Because the ratio of carbon to titanium in the carbide formed by SHS is observed to be 0.84, unreacted carbon should exist in the nickel phase. If every carbon atom is dissolved into nickel, the corresponding atomic per cent of carbon in nickel is 13.8 at % which is beyond the maximum solubility of carbon in nickel. Accordingly, the gamma γ-phase is assumed to be saturated with carbon. Actually, the γ-phase may contain a maximum amount of carbon due to the fast-moving combustion front and fast cooling rates. With this assumption, the lattice parameter of nickel saturated with carbon is 0.35432 nm, which is also below the observed value. Hence, it can be concluded that both carbon and titanium existed in the nickel matrix. This causes a peak broadening and phase shift for nickel peaks, as shown in Fig. 2.

3.2. Densification of TiC_x–Ni composites during liquid-phase sintering

Fig. 3 shows micrographs of TiC_x–50 wt % Ni composites liquid-infiltrated at 1500 °C for 3 h. Fig. 4 shows micrographs of TiC_x–50 wt % Ni composites which were liquid-phase sintered at 1500 °C for various times. The titanium carbide particles were irregularly round and were separated from each other by the nickel matrix. Coarsening of carbide grains was observed after sintering at 1500 °C for 3 h. In order to describe quantitatively the microstructural changes, contiguity, volume fraction of carbide phase and carbide particle distribution were measured. The average carbide diameter increased from 4.18 μm to 7.18 μm after liquid-phase sintering at 1500 °C for 3 h; however, contiguity of the samples decreased from 0.21 to 0.16. It is clear that as the sintering time increases, carbide grains grow and contiguity decreases. Compared with the initial titanium carbide size, the average diameter of the titanium carbide after liquid-phase sintering becomes smaller than the value of the initial carbide size (11.4 μm) before liquid-phase sintering. This means that titanium carbide dissolves into nickel during the solution–precipitation stage of liquid-phase sintering.

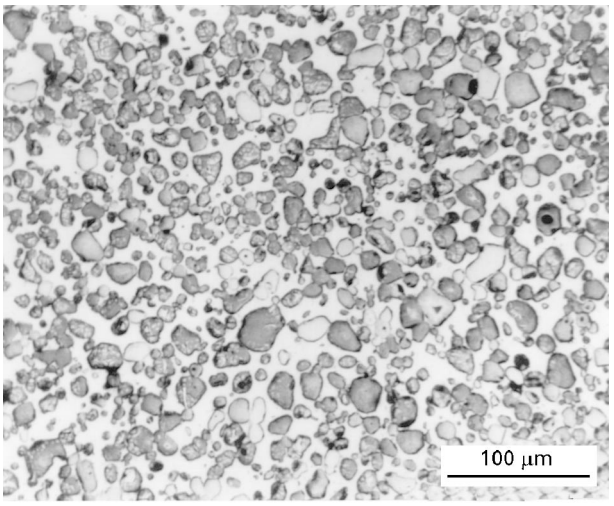

Figure 3 Micrograph of $TiC_{0.87}$–50 wt % Ni liquid-infiltrated at 1500 °C for 3 h.

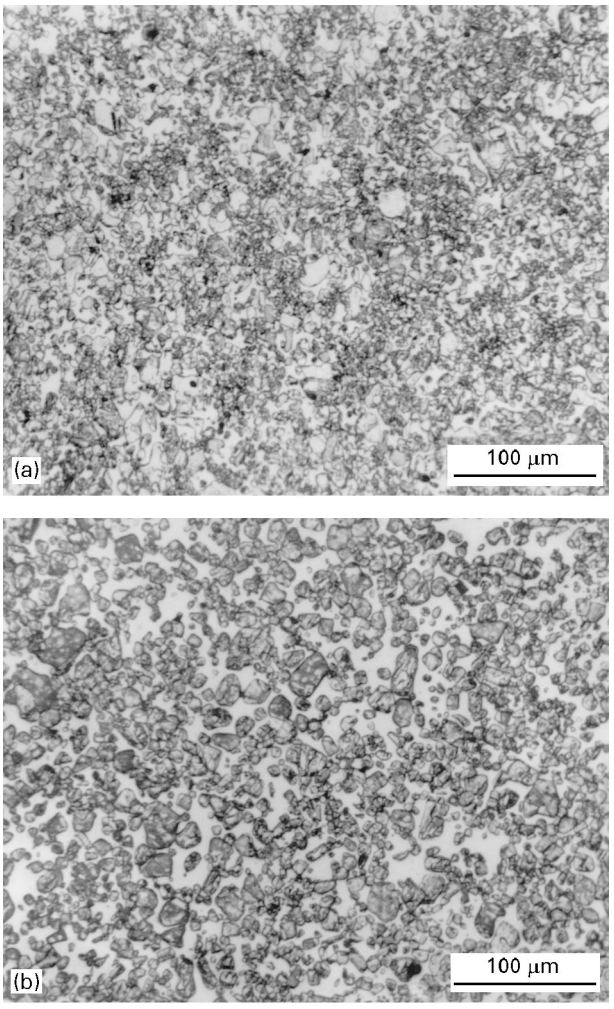

Figure 4 Micrographs of $TiC_{0.87}$–50 wt % Ni liquid-phase sintered at 1500 °C for (a) 10 min, and (b) 3 h.

To study the densification behaviour of a TiC_x–Ni compact during liquid-phase sintering, the absolute density was measured by a helium gas autopycrometer. Fig. 5 shows the initial stage of densification of TiC_x–50 wt % Ni compacts versus sintering temperature for three different concentrations after

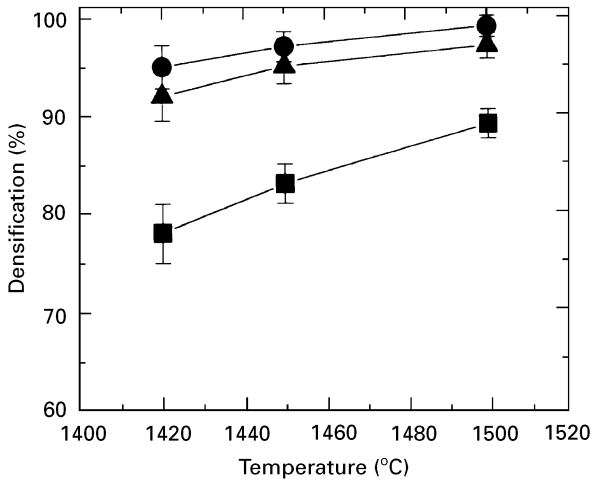

Figure 5 Densification of TiC_x–50 wt % Ni after sintering at each temperature for 10 min. (●) $TiC_{0.79}$–50 wt % Ni, (▲) $TiC_{0.87}$–50 wt % Ni–1.08 wt %, (■) $TiC_{0.84}$–50 wt % Ni–1.34 wt %.

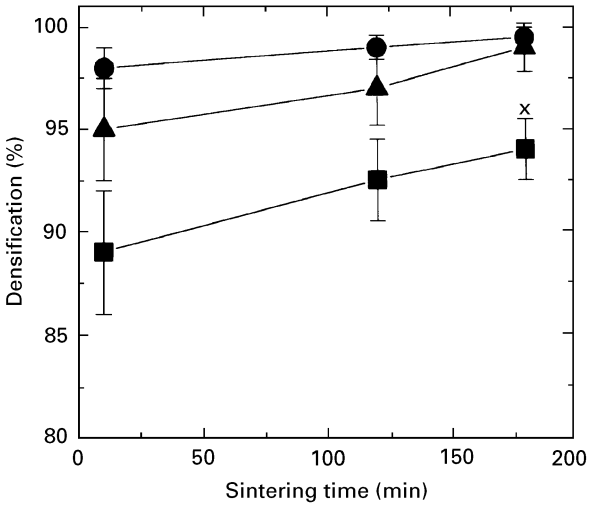

Figure 6 Densification of TiC_x–50 wt % Ni versus sintering time at 1500 °C. (●) $TiC_{0.79}$–50 wt % Ni, (■) $TiC_{0.84}$–1.34 wt % C–50 wt % Ni, (▲) $TiC_{0.87}$–1.08 wt % C–50 wt % Ni, (×) $TiC_{0.87}$–1.08 wt % C–50 wt % Ni (infiltrated).

10 min at each temperature. It was observed that higher sintering temperatures are required to obtain an equivalent degree of densification as the carbon content in nickel is increased. Fig. 6 shows the effect of sintering time on the sintered density of TiC_x–Ni composites. The densities of the liquid-phase sintered sample were 94%–97% theoretical density. The corresponding liquid-phase infiltrated sample was about 94% theoretical density, slightly less than that of a liquid-phase sintered sample.

Although systems with a high solubility, such as TiC–Ni, are often able to obtain a full density in approximately 20 min [13], densities of only 90% theoretical density were obtained after approximately 1 h for the samples with high carbon contents. These indicate that the densification rates are faster for systems with lower carbon content. This sintering behaviour can be explained with the composition change and the wettability change due to the additional carbon. Liquid-phase densification of titanium carbide–nickel composites is strongly dependent upon the composition of the system [15]. In this study, titanium carbides were prepared through the combustion reaction, and these titanium carbide-nickel composites contained unreacted carbons. Therefore, the sintering mechanism can be better understood through an examination of a titanium–nickel–carbon ternary system.

TABLE III Constant temperature solidus equilibra [15, 16]

Binary equilibrium	Temp. (°C)	Ternary equilibrium	Temp. (°C)
L/γ	1455	$L/(\gamma + \delta)$	1307
$L/(\gamma + C)$	1328	$L/(\gamma + \delta + C)$	1270
$L/(\gamma + TiNi_3)$	1304	$L/(\gamma + \delta + TiNi_3)$	1295
$L/(TiNi_3)$	1380	$(L + \delta)/TiNi_3$	1390
$L/(TiNi_3 + TiNi)$	1120	$L/(TiNi_3 + TiNi + \delta)$	1120
L + TiNi	1310	$(L + \delta)/TiNi$	> 1275
$(L + TiNi)/Ti_2Ni$	984	$(L + TiNi + \delta)/Ti_2Ni$	1050
$L/(Ti_2Ni + \beta)$	942	$(L + \delta)/(Ti_2Ni + \beta)$	980

The Ti–Ni–C pseudo-ternary phase diagram was studied by Stover and Wulff and others [15, 16]. The ternary diagram is complicated by a number of intermetallics in the titanium–nickel system and a wide composition range of the carbide. Stover and Wulff measured a slight increase in the lattice parameter of carbide melt in the presence of nickel alloy and reported that the solubility is not above a fraction of an atomic per cent [15]. Ternary eutectics occur on either side with TiNi or with carbon. Table III lists various isothermal reactions determined by Stover and Wulff, where γ is the nickel-rich solution, and δ is a carbide phase. Each of the titanium–nickel intermetallics is in equilibrium with a δ carbide phase. The equilibrium composition slightly changes with the carbon content of the carbide. The solubility of nickel in titanium carbide is not known to have been determined.

The carbon analysis of the titanium carbides from this study indicated the approximate compositions, $TiC_{0.84}$ (17.4 wt % C, 45.6 at % C), $TiC_{0.87}$ (17.9 wt % C, 46.5 at % C) and $TiC_{0.79}$ (16.5 wt % C, 44.1 at % C), because the total carbon contents of $TiC_{0.84}$–50 wt % Ni–1.34 wt % C, $TiC_{0.87}$–50 wt % Ni–1.08 wt % C and $TiC_{0.79}$–50 wt % Ni are 32.7, 30.1 and 28.6 at % C, respectively. The densification behaviour for three compositions is shown in Figs 5 and 6. The changes in carbon content result in different equilibrium phase relationships for these samples. These changes can directly influence liquid-phase sintering behaviour. Hence, the excess carbon effect on the densification behaviour during liquid-phase sintering can be discussed on the basis of the titanium–nickel–carbon phase relationship. Fig. 7 shows the trace of liquidus lines for the compositions A and C, to illustrate the liquid formation during liquid-phase sintering [17]. The composition of $TiC_{0.84}$–50 wt % Ni–1.34 wt % C is in the region of ternary $C + \gamma + \delta$ (point A in Fig. 7). Upon heating,

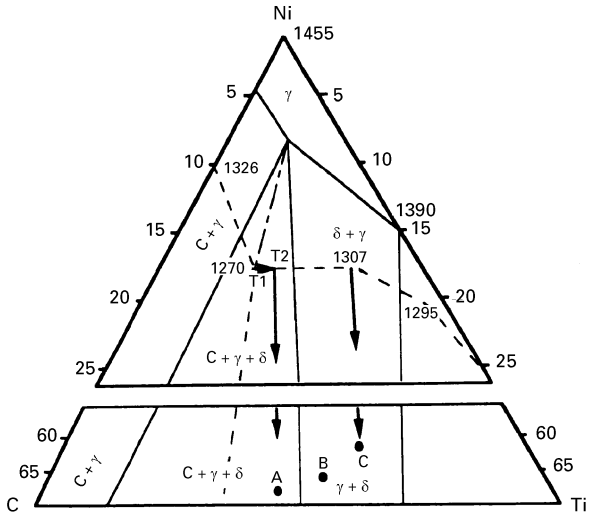

Figure 7 Schematic liquidus line traces with increasing temperature for the compositions of $TiC_{0.84}$–50 wt % Ni and $TiC_{0.84}$–50 wt % Ni–1.34 wt % C (note, both triangles have different magnitudes).

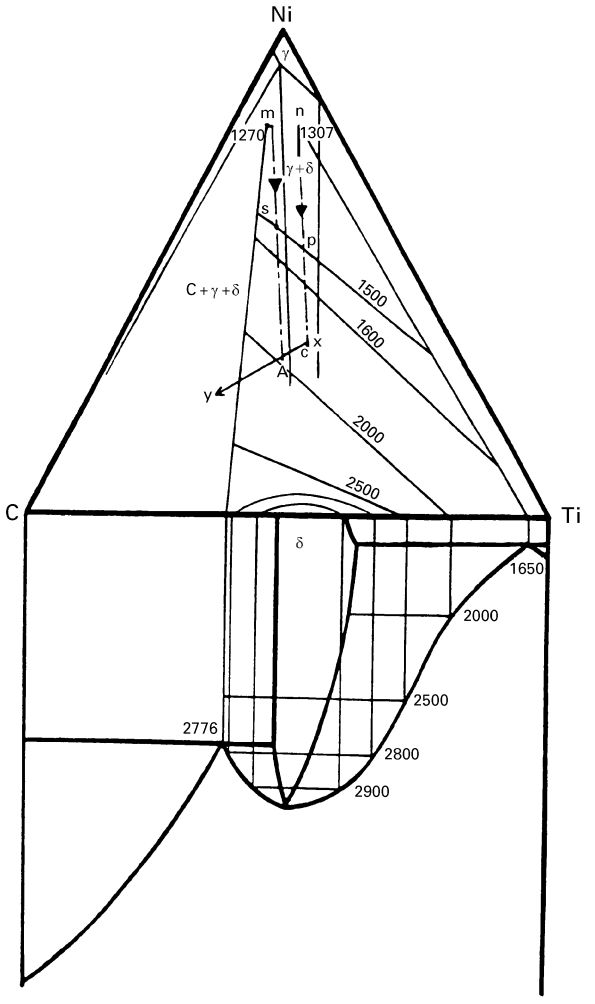

Figure 8 Schematic liquidus isotherms for the δ-liquid region.

liquid will form in equilibrium with carbon and a carbon-rich titanium carbide, δ (L = C + γ + δ), at the ternary eutectic temperature of 1270 °C. Above 1270 °C, e.g. at T_1, the composition of the liquid moves away from the ternary eutectic point (1270 °C) towards the quasi-binary eutectic point (L = γ + δ at 1307 °C). As this occurs, the δ-liquid tie line moves across the phase diagram from left to right, eventually including the initial composition (point A) at a temperature of T_2 (1307 °C > T_2 > T_1 > 1270 °C) where no more γ-phase exists. If the composition of δ-phase is relatively constant with temperature, the composition of the liquid moves along the δ-liquid tie line towards the δ-phase, as melting of the δ-phase occurs [17]. At 1500 °C, the composition of the liquid reaches the 1500 °C isotherm on the δ-liquidus surface. The composition of $TiC_{0.84}$–50 wt % Ni (point C in Fig. 8) is in the region of the γ–δ quasi-binary.

Under equilibrium conditions, this composition is expected to form a liquid at the quasi-binary eutectic point (L = γ + δ at 1307 °C). As the temperature increases, the composition of the liquid moves from the quasi-binary eutectic point towards the initial composition at point C [17]. In each case the amount of liquid is given by the lever rule applied to the bulk composition in the δ-liquid-phase field at 1500 °C. The 1500 °C isotherm for the Ti–Ni system is unknown. However, the angle of the 1500 °C δ-liquidus contour with respect to the C–Ti binary over the composition range from point A to point C, can be estimated by drawing δ-liquidus isotherms based on the Ti–C binary and the Ti–C–Ni ternary equilibrium phase diagrams. The eutectic points of carbon–titanium carbide and titanium carbide are 2776 and 1650 °C respectively [2], and a quasi-binary eutectic point between γ and δ and ternary eutectic point involving graphite occur at 1307 and 1270 °C, respectively [12]. The δ-liquidus surface is the surface including these eutectic points. To simplify drawing δ-liquidus contours, the effects of the ternary equilibria and binary equilibria with titanium nickel compounds other than $TiNi_3$ were assumed negligible in the composition range of A and C. Fig. 8 shows the δ-liquidus surface and the corresponding δ-isotherms. The L = δ + C and L = δ + γ liquid boundary curves were drawn. Points m and n are the ternary eutectic point (1270 °C) and quasi-binary eutectic point (1307 °C), respectively. As carbon content increases, the composition moves from Point x to Point **y**. As shown in Fig. 8 the 1500 °C δ-liquidus isotherm is expected to be a downward slope running through points s and p, lying at an angle intermediate between the C–Ti binary and the Ti–Ni binary. The compositions of liquid for the initial compositions of A and C reach points s and p at 1500 °C in Fig. 8, respectively. If this is true, the amount of liquid in composition A is always less than that in composition C at 1500 °C. Hence the presence of excess carbon in equilibrium with the liquid and carbide phases should greatly inhibit densification.

The wettability change due to the excess carbon can also influence the liquid-phase sintering behaviour, especially the first and second stages of liquid-phase sintering, because the surface free-energy of a particulate system is varied at a high temperature in the presence of a liquid-phase during liquid-phase sintering. Wetting at high temperatures is an extremely complicated phenomenon in which chemical reactions between different phases play an important role [18].

The wettability of titanium carbide by nickel in various atmospheres was studied by Humenik and Perikh [19]. They measured contact angles of 17°, 30°, and 32° for nickel on titanium carbide at 1450 °C in hydrogen, a vacuum (10^{-5} torr), and helium, respectively. The wetting angle, θ is also strongly dependent upon carbon content in titanium carbide. Ramqvist [20] reported that the contact angle varied from $\theta = 22°$ for $TiC_{1.0}$ to a wetting condition of $\theta = 0°$ for $TiC_{0.49}$. It was found that more stable carbides led to a higher liquid–solid interfacial energy and thus poor wetting. This means that the dissolution of non-stoichiometric titanium carbide, TiC_x, into nickel results in a change of the wetting angle. The carbon content in the liquid phase increases with the dissolution of titanium carbide and the addition of carbon. Exner *et al.* [18, 21] studied the dependence of titanium carbide dissolution on carbon concentration in nickel, where the solubility of carbide in the liquid phase decreased with carbon content in the liquid. Table IV shows literature values for the contact angles of TiC_x alloy system. Carbon in nickel and carbon in TiC_x influence the contact angle. An addition of 2 wt % carbon in nickel increased the contact angle from 22° for pure nickel in titanium carbide, to 80° at 1400 °C in vacuum. Similarly, increasing the carbon in TiC_x results in an increase in the contact angle. The increased contact angle leads to the reduction of the interparticle force acting on solid particles separated by a liquid bridge. Interparticle force plays an important role in the densification during liquid-phase sintering. Considering the three stages of liquid-phase sintering, such as (1) a rearrangement stage, (2) a solution–precipitation stage, and (3) a coalescence stage, generally [23], rapid densification occurs with the formation of a liquid phase during the rearrangement stage. Liquid flow, under the surface force, causes rearrangement of solid particles. For the titanium carbide–nickel system, it is known that an initial shrinkage occurs because the solid titanium carbide is highly soluble in the liquid nickel [22–25]. Because the dissolution of titanium carbide is reduced due to the excess carbon content in nickel, poor wettability is introduced. Accordingly, reduction of interparticle force leads to low densification, especially during the initial stage of densification. This is support for the low densification rates of TiC_x–Ni composites with excess carbon, as shown Figs 5 and 6, being related to the reduction of interparticle force due to the poor wettability. Therefore, the existence of excess carbon, which originated from the SHS product, results in a retarding of the densification of the TiC_x–Ni composites.

TABLE IV Contact angles of titanium carbide-alloy system [14, 18–22]

Substance	Metal or alloy (wt %)	Temp. (°C)	Contact angle (deg)
TiC	Ni	1450/H_2(1 atm)	17
TiC	Ni	1450/vacuum(10^{-3} Pa)	30
TiC	Ni	1400/vacuum(10^{-3} Pa)	32
TiC	Ni	1400/vacuum(10^{-3} Pa)	22
$TiC_{0.49}$	Ni	1400/vacuum(10^{-3} Pa)	0
TiC	Ni–2 wt % C	1400/vacuum(10^{-3} Pa)	80
TiC	Ni–10 wt % Mo	1450/vacuum(10^{-3} Pa)	0
TiC	Ni–10 wt % Ti	1450/vacuum(10^{-3} Pa)	25

4. Conclusions

Densification behaviour of the TiC–Ni system formed by self-propagating high-temperature synthesis reaction was studied to develop fabrication processes of the structural metal-matrix composites. The following points summarize the main findings of this study.

1. TiC_x–50 wt % Ni composites were made through simultaneous self-propagating high-temperature synthesis reaction. The final phases of the products were titanium carbide and nickel-rich solid solution for the initial stoichiometric mixture of titanium and graphite containing 50 wt % nickel. There were no traces of free titanium nor titanium–nickel intermetallic phases remaining after the reaction.

2. The addition of nickel during a combustion reaction of titanium and carbon resulted in decreases of the combustion temperature and combustion rate. From the micrographic observations, the morphologies of the titanium carbide particles were predominantly round and the grains were separated from each other by the nickel matrix.

3. For the composites prepared with a self-propagating high-temperature synthesis reaction followed by liquid-phase sintering and liquid-infiltration, the existence of excess carbon, which originated from the SHS product, results in a decrease of the sintering rate because of the poor wettability and the reduced amount of liquid phase during liquid-phase sintering.

4. The densities of the liquid-phase sintered samples were more than 97% theoretical density. The corresponding liquid-infiltrated sample was 95% theoretical density, slightly less than that of liquid-phase sintered samples.

Acknowledgements

The authors thank their colleagues in the Michigan Technological University for valuable discussion, and the Korea Nuclear Fuel Co. for preparing this manuscript. This work was financially supported by the Research Excellence Fund from the State of Michigan, USA.

References

1. R. K. VISWANADHAQM and J. D. VENABLES, *Metall. Trans.* **8** (1977) 187.
2. Y. M. MAKSIMOV, A. G. MERZHANOV, A. T. PAK and B. S. BRAVERMAN, *Izv. Akad. Nauk. SSR Metall.* **2** (1985) 219.
3. Y. TAEOKA, O. ODAQARA and Y. KAIEDA, *J. Amer. Ceram. Soc.* **72** (1989) 1047.
4. Z. A. MUNIR, *Ceram. Bull.* **67** (1988) 342.
5. S. D. DUNMEAD, D. W. READEY, C. E. SEMELER and J. B. HOLT, *J. Amer. Ceram. Soc.* **11** (1984) c 224.
6. F. V. LENEL, "Powder Metallurgy Principles and Applications" (Princeton, NJ, 1980) p. 313.
7. J. WAMBLOD, "Cermets" (Reinhold, New York, 1960) p. 112.

8. M. GERMAN, "Liquid Phase Sintering" (Plenum Press, New York, London, 1985) p. 160.
9. B. MEREDITH and D. R. MILNER, *Powder Metall.* **3** (1976) 162.
10. Y. CHOI, M. E. MULLINS, K. WIJAYATILEKE and J. K. LEE, *Metall. Trans.* **23A** (1992) 2387.
11. O. ODAWARA and Y. KAIEDA, *J. Jpn Soc. Technol. Plast.* **28** (1987) 3.
12. E. T. TURKDOGAN, R. A. HANCOCK, and S. I. HERLITZ, *J. Iron Steel Inst.* **182** (1956) 274.
13. M. F. SINGLETON and P. NASH, in "Phase Diagram of Binary Nickel Alloys" (ASM, Metal Park, OH, 1981) p. 50.
14. K. TAHTINEN and M. H. TIKKANEN, *Int. J. Powder Metall.* **17** (1979) 80.
15. E. R. STOVER and J. WULFF, *Trans. Metall. Soc. AIME* **215** (1959) 127.
16. V. N. EREMENKO and Z. I. TOLMACHEVA, *Poroshkovaya Metall* **2** (1961) 21.
17. D. J. MILLER and J. A. PACK, *J. Amer. Ceram. Soc.* **66** (1983) 841.
18. H. E. EXNER, E. SANTA MARTA, and G. PETZOW, in "Modern Developments in Powder Metallurgy", April 1971, edited by H. H. Hausner (Plenum Press, New York, London, 1971) p. 315.
19. M. HUMENIK Jr and N. M. PARIKH, *J. Amer. Ceram. Soc.* **39** (1956) 60.
20. L. RAMQVIST, *Int. J. Powder Metall.* **1** (1962) 2.
21. J. C. VIALA, C. VINCENT, and H. VINCENT, *Met. Res. Bull.* **25** (1990) 457.
22. W. J. HUPPMAN, *Mater. Sci. Res.* **10** (1979) 257.
23. W. D. KINGERY, *J. Appl. Phys.* **30** (1959) 301.
24. G. H. GISSINGER, H. F. FISCHMESTER, H. L. LUKAS, *Acta Metall.* **21** (1973), 715.
25. S. YAMADA, *J. Powder Metall.* **8** (1969) 190.

Received 7 May
and accepted 17 September 1996